

Computational and experimental exploration of the gas-phase chemistry of alkyloxalate ions

ROCOCOO⁻ (R = H, CH₃, C₂H₅, *i*-C₃H₇, and *t*-C₄H₉)

Héloïse Soldi-Lose^a, Detlef Schröder^b, Helmut Schwarz^{a,*}

^a *Institut für Chemie der Technischen Universität Berlin, Straße des 17. Juni 135, 10623 Berlin, Germany*

^b *Institute of Organic Chemistry and Biochemistry, Academy of Sciences of the Czech Republic, Flemingovo nám. 2, 16610 Prague 6, Czech Republic*

Received 14 August 2007; received in revised form 14 September 2007; accepted 14 September 2007

Available online 29 September 2007

Abstract

Alkyloxalate ions ROCOCOO⁻ (R = H, CH₃, C₂H₅, *i*-C₃H₇, and *t*-C₄H₉) are investigated by experiment and theory. Computational studies at the MP2/6-311++G(3df,3pd)//MP2/6-311++G(d) level of theory show that the structures vary with changing the size of the alkyl substituent R. Metastable ion and collisional activation mass spectra reveal three decomposition pathways of alkyloxalate ions corresponding to losses of CO and CO₂ as well as a combined expulsion of CO and CO₂. Decarbonylation dominates the spectra by far and leads to the corresponding alkylcarbonate ions ROCOO⁻. Two mechanisms are envisaged to understand this dissociation, and calculations suggest that the reaction proceeds through the formation of an intermediate ion–neutral complex.

© 2007 Elsevier B.V. All rights reserved.

Keywords: Ab-initio calculations; Alkyloxalate; Carbon oxide; Decarbonylation; Mass spectrometry

1. Introduction

The unimolecular reactivity of gaseous organic anions is much less often investigated compared to cations because anionic species are more difficult to generate and frequently do not show interesting decomposition features, as for example rearrangements [1]. Nevertheless, knowledge of the gas-phase behavior of such species can provide useful information for the understanding of reactions occurring in unusual environments, as for instance, in the higher terrestrial atmospheres or in the atmospheres of other planets and moons. In a project dealing with organic compounds of potential interest with respect to the atmosphere of Mars, we have inter-alia focused our attention to a series of alkyloxalate ions (Scheme 1), which are derived from carbon dioxide, the major component of the martian atmosphere. Quite surprisingly, only very little is known about the structures as well as about the dissociation of metastable oxalate ions in the gas phase. Accordingly, here we present a systematic

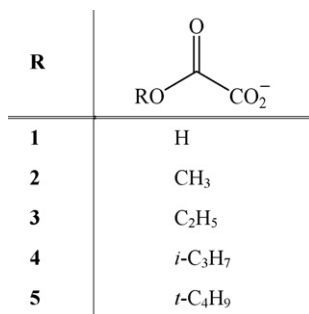
study of the structures and of the dissociation behavior of some representative alkyloxalate ions.

Theory and experiment have been combined to probe and understand the unimolecular dissociations of the anions whose structural minima have been determined by ab-initio methods. Hence, alkyloxalate ions have been generated by negative ion chemical ionization (NICI) and the mass-selected ions have been submitted to metastable ion (MI) and collisional activation (CA) experiments. Because monoalkyloxalates possess several internal rotors, these anions may exist in different conformational structures, and the structures and energetics of different conformers have been determined at the MP2/6-311++G(3df,3pd)//MP2/6-311++G(d) level of theory as well as those of the transition structures involved in the course of decomposition of the anions.

2. Experimental and computational details

The experiments were carried out with a modified VG ZAB/HF/AMD 604 four sector mass spectrometer of BEBE configuration (B stands for magnetic and E for electric sec-

* Corresponding author. Tel.: +49 30 31423483; fax: +49 30 31421102.
E-mail address: Helmut.Schwarz@mail.chem.tu-berlin.de (H. Schwarz).



Scheme 1. Alkyloxalate ions investigated in this work.

tor) which has been described previously [2]. Monoalkyloxalate anions were obtained from the corresponding dialkyloxalates, which are commercially available. Ca. 3 μ L of the precursor were introduced to a chemical ionization (CI) source [3] in the presence of an excess of N₂O serving as a reagent gas and ionized by electrons having a kinetic energy of 100 eV at a repeller voltage of about 0 V. Due to the excess of N₂O, the formation of alkyloxalate ions from the corresponding dialkyloxalates is likely to involve the reaction $N_2O + e^- \rightarrow N_2 + O^{\bullet-}$ as a first step, followed by a formal S_N2 reaction with the ester, $ROCCOOR + O^{\bullet-} \rightarrow ROCCOO^- + RO^{\bullet}$ (see Ref. [4] and references therein, and Ref. [5]); for bulky substituents R, also E2 eliminations are likely to be involved in the ion formation.

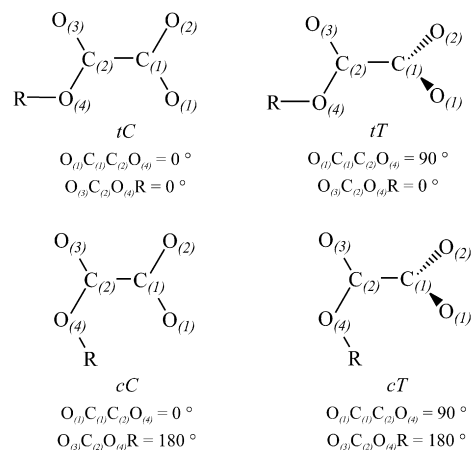
After acceleration to 8 keV kinetic energy, the ions were mass-selected with B(1). Unimolecular fragmentations of metastable ions (MI) occurring in the field-free region (ffr) preceding E1 were recorded by scanning this sector, as well as dissociation of collisionally activated ions (CA) for which a collision cell located in the ffr before E1 was filled with helium (80% transmission, *T*). The data given below are averages of at least three independent measurements.

In the theoretical studies, the geometry optimizations were carried out with the MP2 method [6] using 6-311++G(d) [7,8] basis sets within the GAUSSIAN 03 suite of programs [9]. Stationary points were characterized as minima (no imaginary frequencies) or as transition structures (one imaginary frequency). The calculated frequencies were also used to determine zero point vibrational energies. Those are required for the zero-point corrections of the electronic energies and were scaled by a uniform factor of 0.9496 [10]. Refined energies were then obtained for the optimized geometries in single-point calculations employing the MP2 method in conjunction with 6-311++G(3df,3pd) basis sets [8,11].

3. Results and discussion

3.1. Structures of alkyloxalates

The structure of oxalic acid already has formed the subject of many investigations, particularly because it is one of the simplest examples of a molecule possessing three internal rotors [12–17]. It can indeed exhibit internal rotation around the central carbon–carbon bond connecting the two carbonyl groups and around the two C–OH bonds. In contrast, the structures

Scheme 2. The four conformations of alkyloxalates anions ROCOCOO⁻ (R = H, CH₃, C₂H₅, *i*-C₃H₇, and *t*-C₄H₉) for limiting values of the dihedral angles $O_{(1)C_{(1)}C_{(2)}O_{(4)}}$ and $O_{(3)C_{(2)}O_{(4)}}$.

of deprotonated oxalic acid, i.e., the hydrogen oxalate anion **1**, as well as the monoalkyloxalates ROCOCOO⁻ have been investigated in much less detail. These anions may potentially also exist in different conformations and the determination of the conformational minimum is not obvious as will be shown below. Hence, we have investigated the different conformational structures of alkyloxalates ROCOCOO⁻ for R = H, CH₃, C₂H₅, *i*-C₃H₇, and *t*-C₄H₉. The four conformers, which correspond to the limits of the two relevant dihedral angles, are presented in Scheme 2. Here, the symbols *C* and *T* refer to the conformation of the dihedral angle $O_{(1)C_{(1)}C_{(2)}O_{(4)}}$, whereas the conformers involving rotations of the C₍₂₎–O₍₄₎ bond (i.e., the dihedral angle $O_{(3)C_{(2)}O_{(4)}}$) are denoted by *c* and *t* (here, *c* and *C* stand for *cis*, *t* and *T* for *trans* respectively) [14]. The most relevant features of the optimized geometries of the alkyloxalates **1–5** in these four conformations are given in Table 1.

The analysis of the optimized structural parameters presented in Table 1 reveals changes of bond lengths and angles of alkyloxalates between the various conformations. Rotation around the central C₍₁₎–C₍₂₎ bond (conformers *C* and *T*) induces a minor decrease of the C₍₁₎–O₍₂₎ bond length when passing from the *T* to the *C* conformation. This difference is moderate for the small substituents R (ca. 0.010 Å for R = H and ca. 0.007 Å for R = CH₃) and decreases even further for larger ones (ca. 0.005 Å for R = C₂H₅, *i*-C₃H₇, and *t*-C₄H₉). In marked contrast, much more pronounced changes occur for the C₍₁₎–C₍₂₎ bond length, for which a passage from the *T* to the *C* conformation leads to bond elongations of about 0.045 Å. This increase may be explained by steric constraints due to the “planar” backbone structure of the *C* conformation. The same reasoning also explains the difference of the O₍₄₎–R bond lengths observed between the *cT* and *tT* conformers and between the *cC* and *tC* structures with an average elongation of 0.005 Å in the *c* conformers. The R groups of these conformers present indeed some proximity to the carbonyl group O_{(1)C₍₁₎O₍₂₎}, which may hinder it to be favorably positioned for small O₍₄₎–R bond lengths. An elongation of the O₍₄₎–R bond is accordingly observed to allow a good spatial organization of the R group. For another

Table 1
Selected bond lengths (in Å) and bond angles (in °) of the alkyloxalates **1–5** in the four conformations investigated at the MP2/6-311++G(d) level of theory

		C ₍₁₎ O ₍₁₎	C ₍₁₎ O ₍₂₎	C ₍₁₎ C ₍₂₎	C ₍₂₎ O ₍₃₎	C ₍₂₎ O ₍₄₎	O ₍₄₎ R	O ₍₁₎ C ₍₁₎ O ₍₂₎	O ₍₃₎ C ₍₂₎ O ₍₄₎
1	<i>tT</i>	1.252	1.252	1.541	1.219	1.372	0.970	132.4	120.0
	<i>cT</i>	1.255	1.255	1.546	1.210	1.384	0.966	128.3	118.8
	<i>cC</i>	1.273	1.238	1.584	1.212	1.355	0.988	127.3	122.1
	<i>tC</i>	1.250	1.249	1.584	1.218	1.370	0.969	132.4	119.5
2	<i>tT</i>	1.253	1.253	1.540	1.218	1.373	1.424	132.2	121.1
	<i>cT</i>	1.255	1.253	1.546	1.213	1.380	1.431	131.7	117.7
	<i>cC</i>	1.257	1.243	1.597	1.212	1.380	1.430	131.4	115.4
	<i>tC</i>	1.251	1.250	1.584	1.217	1.370	1.422	132.1	120.6
3	<i>tT</i>	1.254	1.253	1.540	1.218	1.375	1.430	132.2	121.6
	<i>cT</i>	1.256	1.253	1.545	1.213	1.381	1.436	132.1	117.7
	<i>cC</i>	1.257	1.243	1.598	1.212	1.382	1.435	131.4	115.5
	<i>tC</i>	1.251	1.250	1.584	1.217	1.372	1.426	132.1	120.7
4	<i>tT</i>	1.254	1.254	1.540	1.219	1.372	1.441	132.1	122.5
	<i>cT</i>	1.257	1.251	1.546	1.215	1.381	1.446	131.2	116.4
	<i>cC</i>	1.256	1.244	1.593	1.211	1.390	1.444	131.3	116.1
	<i>tC</i>	1.251	1.250	1.586	1.217	1.369	1.439	132.0	121.9
5	<i>tT</i>	1.254	1.254	1.541	1.218	1.373	1.448	132.2	122.9
	<i>cT</i>	1.251	1.251	1.546	1.214	1.384	1.453	131.2	116.1
	<i>cC</i>	1.251	1.244	1.594	1.214	1.384	1.453	131.2	116.1
	<i>tC</i>	1.254	1.250	1.588	1.218	1.373	1.448	132.2	122.9

reason, this increase is particularly important for the hydrogen oxalate ion when passing from the *tC* to the *cC* conformation (+0.019 Å). This latter conformation is indeed strongly stabilized through an intramolecular hydrogen bond (see below) what implies a rapprochement of the hydrogen to the O₍₁₎ atom. Further, as for the O₍₄₎R bond, a slight increase of the C₍₁₎–O₍₁₎ bond length is observed when changing from the *t* to the *c* conformation. The C₍₂₎–O₍₃₎ and C₍₂₎–O₍₄₎ distances are also influenced by a rotation around the C₍₂₎–O₍₄₎ axis. Again, both bonds are slightly longer in the *c* than in the *t* conformation. Concerning the angles, one notices that the O₍₁₎C₍₁₎O₍₂₎ angle remains almost unchanged for the various conformers, except for the hydrogen oxalate ion which presents a structure more “opened” by ca. 4° in the *c* conformation compared to the *t* one. Slightly larger changes are observed for the O₍₃₎C₍₂₎O₍₄₎ angle which decreases by ca. 6° when passing from the *t* to the *c* configuration. To summarize, if one roughly compares the different conformational structures predicted by theory, it can be seen that if the central backbone is planar (*C*), the structures of alkyloxalates are elongated along the C₍₁₎–C₍₂₎ axis. The most compact structure corresponds to the *cT* conformation and the loosest one to the *tT* conformation.

The total electronic and relative energies of alkyloxalates **1–5** calculated at the MP2/6-311++G(3df,3pd) level of theory for the four optimized conformational structures are given in Table 2. The number of imaginary frequencies is also included as they allow the characterization of the conformers as minima or as transition structures.

A comparison of the energetics of the four conformers of the alkyloxalates **2–5** shows that the planar conformers *cC* and *tC* correspond to transition structures, whereas the non-planar structures *cT* and *tT* are minima. A more detailed discussion for each alkyloxalate will be presented after the examination of the particular case of the hydrogen oxalate ion. The ion with R = H

Table 2
Total energies E_{tot} (in Hartrees, H)^a, relative energies E_{rel} (in kcal/mol)^b, and number of imaginary frequencies of the four conformers of the alkyloxalates **1–5** according to MP2/6-311++G(3df,3pd)/MP2/6-311++G(d) calculations

	Conformer	E_{tot} ^a (H)	E_{rel} ^b (kcal/mol)	Number of imaginary frequencies
1	<i>tT</i>	–377.1981850	8.9	0
	<i>cT</i>	–377.1968332	9.8	1
	<i>cC</i>	–377.212433	0.0	0
	<i>tC</i>	–377.1930629	12.2	1
2	<i>tT</i>	–416.3727241	0.3	0
	<i>cT</i>	–416.3732318	0.0	0
	<i>cC</i>	–416.3690674	2.6	1
	<i>tC</i>	–416.3645157	5.5	1
3	<i>tT</i>	–455.5723569	0.5	0
	<i>cT</i>	–455.5731566	0.0	0
	<i>cC</i>	–455.5688245	2.7	1
	<i>tC</i>	–455.5649954	5.1	1
4	<i>tT</i>	–494.7701893	0.0	0
	<i>cT</i>	–494.7693479	0.5	0
	<i>cC</i>	–494.7596878	6.6	1
	<i>tC</i>	–494.765386	3.0	1
5	<i>tT</i>	–533.9737309	0.0	0
	<i>cT</i>	–533.9731006	0.4	0
	<i>cC</i>	–533.9634608	6.4	1
	<i>tC</i>	–533.9700754	2.3	1

^a ZPE included and uniformly scaled (0.9496).

^b The energy is given relative to the most stable conformer for each alkyloxalate.

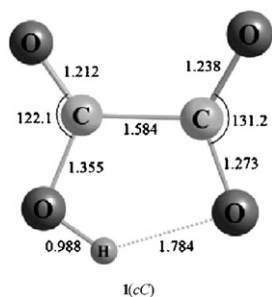


Fig. 1. Optimized structure of the most stable conformer of the hydrogen oxalate ion **1** at the MP2/6-311++G(d) level of theory.

differs from the other ROCOCOO[−] anions studied because the conformation *cC* possesses an intramolecular hydrogen bond between two oxygen atoms (Fig. 1). The resulting overall stabilization of this structure amounts to ca. 10 kcal/mol compared to the other conformers (Table 2). Furthermore, frequency calculations characterize the *tT* conformer as a minimum and the *cT* and *tC* conformers as transition structures. The results concerning the relative energies of the conformers as well as their characterization as minima or saddle points are in complete agreement with the findings of Cheng and Shyu [18] in which the four conformations of the hydrogen oxalate ion were considered at various levels of theory.

As already mentioned, the conformations *cT* and *tC* correspond to transition structures for HOCOCOO[−], and the normal modes associated to the imaginary frequency of each conformer are associated with torsions around both the C₍₁₎–C₍₂₎ and C₍₂₎–O₍₄₎ axis. A schematic description showing the conformational connections between the relevant conformers of the hydrogen oxalate ion is presented in Fig. 2.

The conformational structures **1(cT)** and **1(tT)** differ by only 0.9 kcal/mol, and Cheng and Shyu [18] even found the transition structure **1(cT)** to be 0.4 kcal/mol lower in energy than the local minimum **1(tT)**. Nevertheless, the most favorable conformer **1(cC)** is clearly lower in energy than all other conformational structures investigated and is accordingly assumed as the most stable conformer of the ion **1**.

Concerning the four other alkyloxalates investigated, energy calculations show that all conformers *cC* and *tC* correspond to

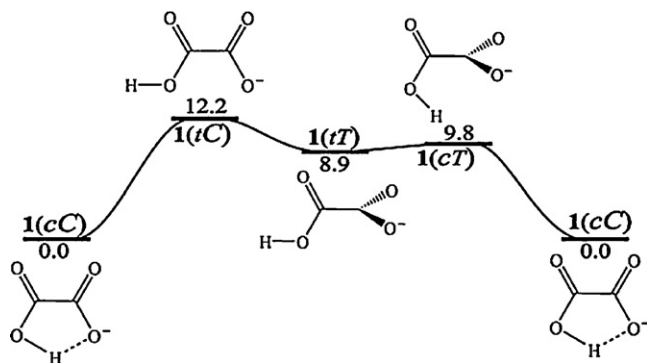
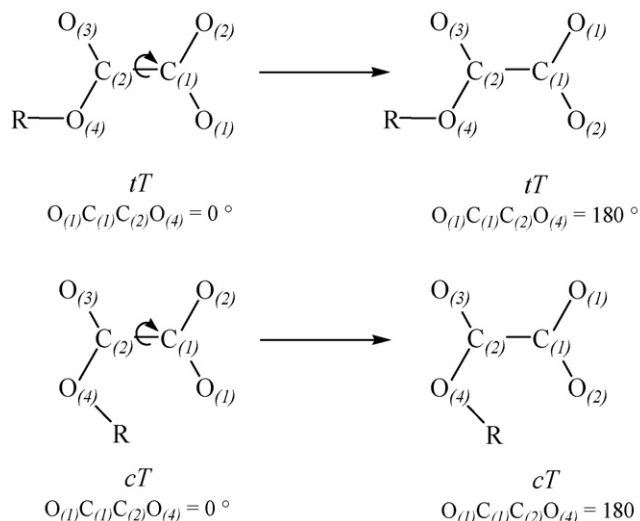


Fig. 2. Connections between the different conformers of the hydrogen oxalate ion **1** according to MP2/6-311++G(3df,3pd)//MP2/6-311++G(d) calculations (energies in kcal/mol).



Scheme 3. The conformational structure of alkyloxalates ROCOCOO[−] (R = H, CH₃, C₂H₅, *i*-C₃H₇, and *t*-C₄H₉) is conserved by rotation of 180° around the C₍₁₎–C₍₂₎ axis due to the symmetry of the carboxylate group.

transition structures, while the *tT* and *cT* conformers are minima. For methyl- and ethyl oxalate ions, the most stable structure is the conformation *cT* whereas for *i*-propyl- and *t*-butyl oxalate, it is the conformation *tT* (Fig. 3).

The connections between the various conformers of the alkyloxalates **2–5** are not as straightforward as in the case of **1**. An analysis of the normal mode associated to the imaginary frequency of the conformers *cC* and *tC* reveals that these transition structures correspond to rotations around the C₍₁₎–C₍₂₎ axis changing the value of the dihedral angle O₍₁₎C₍₁₎C₍₂₎O₍₄₎ from 0° to 180°. Due to the symmetry of the carboxylate group, these two values of the dihedral angle correspond to the same conformation (Scheme 3).

The passage of the conformation *cT* to *tT* requires a rotation around the C₍₂₎–O₍₄₎ axis to change the dihedral angle O₍₃₎C₍₂₎O₍₄₎R from 180° to 0° (R = CH₃, C₂H₅, *i*-C₃H₇, and *t*-C₄H₉). The transition structure TS(*cT*/*tT*) associated with this rotation has a T-shaped conformation and a dihedral angle O₍₃₎C₍₂₎O₍₄₎R of 90° (R = CH₃, C₂H₅, *i*-C₃H₇, and *t*-C₄H₉). As an example, the optimized structure of the transition structure of the methyloxalate ion **2** is shown in Fig. 4. The relative energies of the transition structures are given in Table 3 for the ions **2–5**.

Table 3

Total and relative energies $E_{\text{tot}}^{\text{a}}$ and $E_{\text{rel}}^{\text{b}}$ (respectively in Hartrees, H and in kcal/mol) of the transition structures TS(*cT*/*tT*) for the alkyloxalates **2–5** obtained at the MP2/6-311++G(3df,3pd)//MP2/6-311++G(d) level of theory

		$E_{\text{tot}}^{\text{a}}$ (H)	$E_{\text{rel}}^{\text{b}}$ (kcal/mol)
TS(<i>cT</i> / <i>tT</i>)	2	−416.3598209	8.4
	3	−455.5603955	8.0
	4	−494.7614792	5.5
	5	−533.9652372	5.3

^a ZPE included and uniformly scaled (0.9496).

^b Energies given relative to those of the corresponding alkyloxalates (Table 2) in the most stable conformation (*cT* or *tT*).

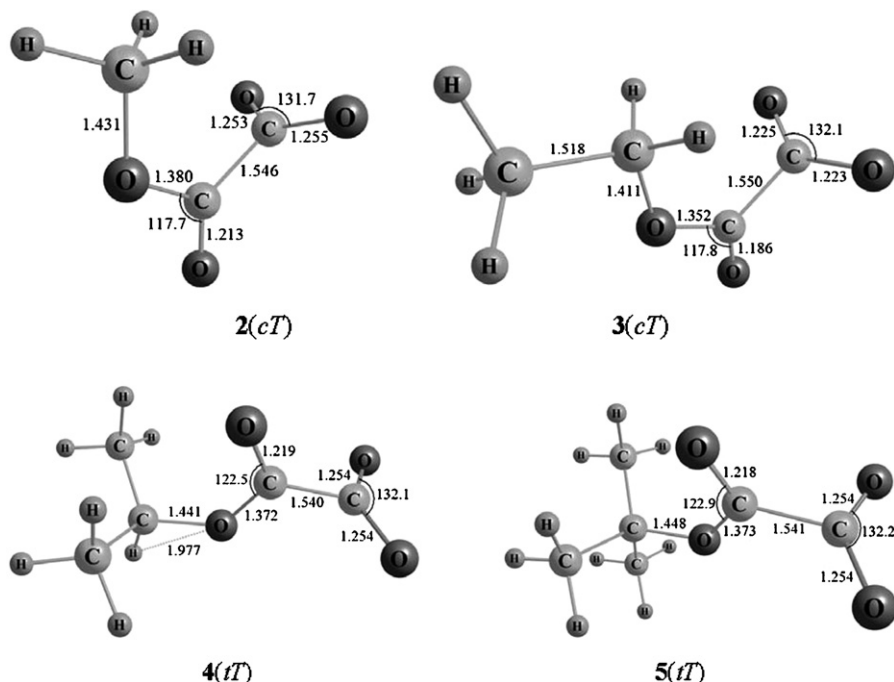


Fig. 3. The most stable conformational minima of the alkyloxalates anions 2–5 obtained at the MP2/6-311++G(d) level of theory.

From the energetics data of the TS(*cT*/*tT*) transition structures (Table 3), a general scheme for the conformational changes of the alkyloxalates 2–5 can be deduced. These schemes are presented in Fig. 5a for methyl- and ethyl-oxalate and in Fig. 5b for *i*-propyl- and *t*-butyl oxalate.

3.2. Unimolecular reactivity of alkyloxalate ions

In Table 4, the MI and CA spectra of the alkyloxalate ions are summarized. The alkyloxalate anions 1–5 show a rather similar behavior. Quite surprisingly, all spectra are largely dominated by a signal corresponding to the loss of neutral CO ($\Delta m = 28$). Two minor signals refer to elimination of CO₂ ($\Delta m = 44$) and to the combined loss of CO₂ and CO ($\Delta m = 72$). The spectra are thus exclusively composed by signals corresponding to CO_{*x*} losses ($x = 1, 2$) and no other eliminations able to compete with these processes are observed. Furthermore, almost no drastic changes are associated when the internal energy of the system is increased (CA experiment), in contrast to what

is in general expected in comparing MI and CA processes [19].

The decomposition process corresponding to the combined loss of CO₂ and CO could consist of either a direct or a consecutive loss of the neutral molecules. As only small changes in intensity for this signal are observed between the MI and CA experiments, the second hypothesis seems less likely as an internal energy gain (by collision) of the system should accordingly lead to a higher intensity. While we attribute this reaction to the formation of CO and CO₂, it has to be mentioned that, in principle, it could also correspond to the loss of a genuine neutral C₂O₃ unit. This molecule has already been extensively studied by both experiment and theory [20–25]. Peppe et al. [22] have shown that the most stable structure of neutral C₂O₃, in the singlet multiplicity, corresponds to a van der Waals complex (Scheme 4) which

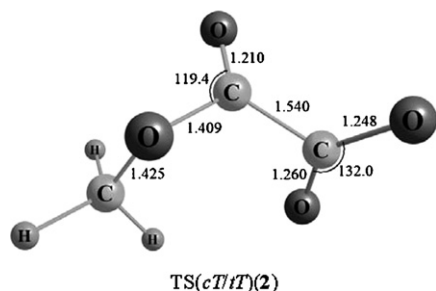


Fig. 4. Optimized transition structure associated to the passage of the *cT* to the *tT* conformation of methyloxalate 2 according to MP2/6-311++G(d) calculations.

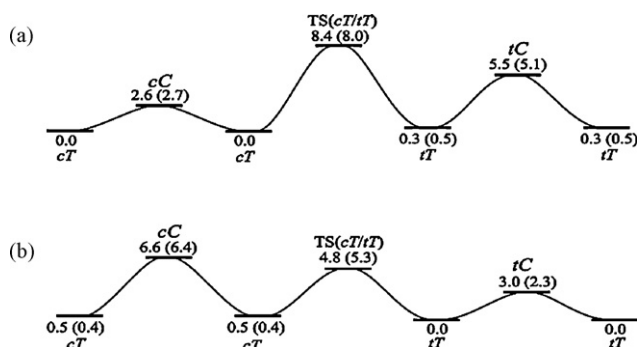


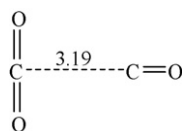
Fig. 5. Conformational interconversion of (a) methyloxalate ions (data for ethyl oxalate in brackets) and (b) *i*-propyl oxalate ions (data for *t*-butyl oxalate in brackets). Energies are given relative to the conformer (a) *cT* of methyl- and ethyl oxalate and (b) *tT* of *i*-propyl- and *t*-butyl oxalate according to MP2/6-311++G(3df,3pd)//MP2/6-311++G(d) calculations (energies in kcal/mol).

Table 4
Intensities^a of fragments in MI and CA spectra of mass-selected alkyloxalates ROCOCOO⁻ (R = H, CH₃, C₂H₅, *i*-C₃H₇, and *t*-C₄H₉)

R (<i>m/z</i>) ^b		-CO	-CO ₂	-(CO + CO ₂)
1: H (89)	MI	100	1	1
	CA	100	2	2
2: CH ₃ (103)	MI	100	1	1
	CA	100	1	2
3: C ₂ H ₅ (117)	MI	100	1	1
	CA	100	2	1
4: <i>i</i> -C ₃ H ₇ (131)	MI	100	3	1
	CA	100	3	2
5: <i>t</i> -C ₄ H ₉ (145)	MI	100	13	0
	CA	100	16	4

^a Intensity relative to the base peak (=100); peaks <1 are neglected.

^b Mass-to-charge ratio of precursor anion in amu.



Scheme 4. Structure of most stable isomer of ¹C₂O₃. The bond length (in Å) is taken from Peppe et al. [22].

is stable with respect to dissociation to CO₂ and CO by only 1.2 kcal/mol (CCSD(T)/aug-cc-pVDZ//B3LYP/6-31G(d) level of theory). For this reason, we assume that if the neutral species with $\Delta m = 72$ correspond to C₂O₃, it seems very likely that it dissociates immediately into CO and CO₂. In the following, we will therefore assume that the mass difference of $\Delta m = 72$ corresponds to the combined formation of CO + CO₂, rather than genuine C₂O₃ [26].

The structure of the product ion and the mechanism by which decarbonylation ($\Delta m = 28$) occurs is not obvious because this fragment cannot be formed in a direct bond cleavage of the anions, as is the case for the decarboxylation or the combined elimination of CO₂ and CO. Nevertheless, the nature of the product ions due to CO loss can be easily probed by MS/MS experiments because their intensities are high enough to allow consecutive mass selection of the alkyloxalates and of the subsequently formed fragment ions.

Table 5
Intensities^a of observed fragments^b in the CA/CA spectra of RCO₃⁻ ions formed from mass-selected alkyloxalates ROCOCOO₂⁻

R	Selection ^{b,c}	<i>m/z</i> ^b (intensity ^a)
H	89/61	17 (100), 60 (80)
CH ₃	103/75	31 (100), 45 (48), 60 (20)
C ₂ H ₅	117/89	43 (6), 45 (100), 60 (5)
<i>i</i> -C ₃ H ₇	131/103	57 (4), 59 (100), 60 (2)
<i>t</i> -C ₄ H ₉	145/117	57 (20), 60 (11), 73 (100)

^a Intensity relative to the base peak (=100).

^b Mass-to-charge ratio in amu.

^c The experiment consists in selecting the precursor ion alkyloxalates with B1 and the resulting charged fragments with E1 while B2 is scanned. The masses indicated correspond to the mass of the alkyloxalate parents and to the mass of the fragment selected with E1.

Table 6
Calculated heats of reaction (in kcal/mol)^a at 298 K of the observed dissociation processes of alkyloxalates 1–5 at the MP2/6-311++G(3df,3pd)/MP2/6-311++G(d) level of theory

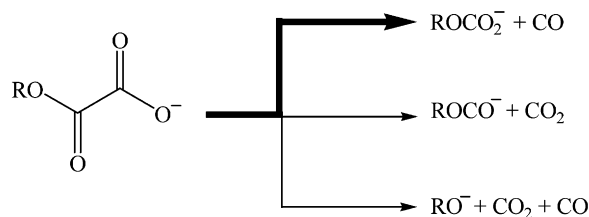
	ROCOO ⁻ + CO	ROCO ⁻ + CO ₂	RO ⁻ + CO + CO ₂
1	17.7	44.9	60.3
2	9.2	35.5	47.0
3	8.7	34.2	43.8
4	5.1	32.5	38.5
5	7.4	31.3	37.6

^a ZPE included and scaled (0.9496).

The loss of CO from the alkyloxalates formally leads to RCO₃⁻ ions with R = H, CH₃, C₂H₅, *i*-C₃H₇, and *t*-C₄H₉. The CA/CA mass spectra of these ions (Table 5) are dominated by signals of the corresponding alkoxide ions RO⁻ (loss of neutral CO₂). A characteristic peak for the loss of alkyl radicals concomitant with the generation of the radical anion CO₃^{•-} (*m/z* = 60) is also present, which indicates that all three oxygen atoms are bound to the same carbon atom. Moreover, in the case of the CH₃CO₃⁻ ion, elimination of formaldehyde concomitant with formation of HCO₂⁻ also takes place. This CA/CA spectrum agrees thus well with the CA spectrum of methylcarbonate given by Hayes et al. [27], as well as the other CA/CA data given in Table 5, with CA experiments of genuine alkylcarbonate ions ROCOO⁻ [28,29]. O'Hair et al. [30] have also investigated the unimolecular reactivity of HOCOCOO⁻ ions and observed a fragment at *m/z* = 61 which they attributed to the hydrogencarbonate ion HOCOO⁻. Consideration of the thermochemistry of the dissociation of the alkyloxalates 1–5 further reveals that the decomposition of alkyloxalate ions into alkylcarbonates and CO is quite favorable, endothermic by only few kcal/mol (Table 6). In comparison, the direct bond cleavages leading to decarboxylation as well as decarboxylation combined with decarbonylation are more than 30 kcal/mol higher in energy. Decarboxylation leads to alkoxy carbonyl anions ROCO⁻, which are well-known species in the gas phase [31,32], and alkoxy anions RO⁻ are obtained by simultaneous loss of CO₂ and CO from alkyloxalates [31,33].

The general dissociation scheme of alkyloxalates can accordingly be summarized by three competing pathways with decarbonylation as the by far major route (Scheme 5).

As far as the direct bond cleavages are concerned, the question of mechanisms is not a burning one. In contrast, decarbonylation of alkyloxalates cannot be understood that easily



Scheme 5. General dissociation scheme of alkyloxalates ROCOCOO⁻ for R = H, CH₃, C₂H₅, *i*-C₃H₇, and *t*-C₄H₉. The bold arrow indicates the main dissociation pathway.

Table 7

Total and relative energies $E_{\text{tot}}^{\text{b}}$ and $E_{\text{rel}}^{\text{c}}$ (respectively in Hartrees, H and in kcal/mol) of the transition states $\text{TS}_{\text{A}}^{\text{a}}$ and $\text{TS}_{\text{B}}^{\text{a}}$ and of the ion–neutral complexes, $\text{INC}_{\text{A}}^{\text{a}}$, involved in the course of decarboxylation of alkyloxalates ROCOCO^- at the MP2/6-311++G(3df,3pd)//MP2/6-311++G(d) level of theory

		$E_{\text{tot}}^{\text{b}}$ (H)	$E_{\text{rel}}^{\text{c}}$ (kcal/mol)
1: H	TS_{A}	−377.1428343	43.7
	INC_{A}	−377.1513545	38.3
	TS_{B}	−377.1044195	67.8
2: CH_3	TS_{A}	−416.3154505	36.3
	INC_{A}	−416.3239468	30.9
	TS_{B}	−416.2786243	59.4
3: C_2H_5	TS_{A}	−455.5148716	36.1
	INC_{A}	−455.5234566	30.7
	TS_{B}	−455.4771170	59.7
4: <i>i</i> - C_3H_7	TS_{A}	−494.7166570	33.6
	INC_{A}	−494.7257410	27.9
	TS_{B}	−494.6574880	70.7
5: <i>t</i> - C_4H_9	TS_{A}	−533.9136187	37.7
	INC_{A}	−533.9236912	31.4
	TS_{B}	−533.8770840	60.6

^a TS_{A} and TS_{B} correspond to the respective transition structures associated with the mechanistic variants **A** and **B** (Scheme 6), and INC_{A} stands for the ion–neutral complex formed prior to decarboxylation.

^b ZPE included and uniformly scaled (0.9496).

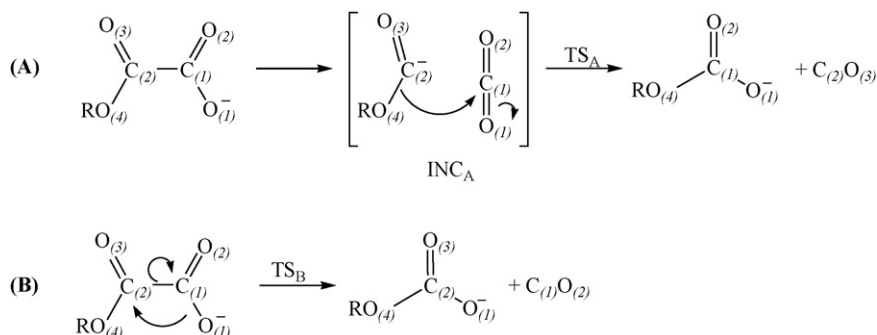
^c Energies are given relative to those of the alkyloxalates (Table 2) in their most stable conformation.

because it requires a rearrangement of the anion; moreover, alkyloxalates possess two different carbonyl groups, which can possibly be eliminated. Two mechanisms appear most plausible (Scheme 6). The first one, denoted as **A**, consists in the formation of an ion–neutral complex $[\text{ROCO}^- \text{CO}_2]$ [34] from the alkyloxalate, followed by an intracomplex attack of carbon dioxide by the nucleophilic oxygen atom $\text{O}_{(4)}$ in the complex (INC_{A}); we note in passing that a scan of the potential energy surface revealed that the formation of INC_{A} proceeds without a barrier. This mechanism has been proposed by O’Hair et al. [30] in the study of dissociation of the hydrogen oxalate ion, but has not been probed any further neither theoretically nor experimentally. The second variant, denoted as **B**, consists in a direct attack of the electrophilic atom $\text{C}_{(2)}$ by the oxygen atom $\text{O}_{(1)}$ carrying the negative charge in alkyloxalate with subsequent elimination of CO. For acid-catalyzed decarboxylation of α -keto carbonic acid involving the carboxyl CO group,

see Ref. [35,36]. Experimentally, these two mechanisms could be probed by means of labeling experiments because the atoms involved are not the same [37]; however a selective synthesis of labeled ions such as $\text{ROC}^{18}\text{OCOO}^-$, $\text{RO}^{13}\text{COCOO}^-$, $\text{ROCOCO}^{18}\text{O}^-$ or $\text{ROCO}^{13}\text{COO}^-$ is far from being trivial and was hence not pursued any further.

Instead, the two mechanisms have been probed computationally. Structures and energies of the transition structures of variants **A** and **B** have been calculated at the MP2/6-311++G(3df,3pd)//MP2/6-311++G(d) level of theory, as well as the ion–neutral complex involved in mechanism **A** for the five alkyloxalates **1–5**. The resulting energies are summarized in Table 7.

In general, the transition structures TS_{A} associated with mechanism **A** are by up to 20 kcal/mol lower in energy than the TS_{B} related to mechanism **B**. Formation of the ion–neutral complex INC_{A} costs on average 30 kcal/mol relative to the alkyloxalates, except for the hydrogen oxalate ion which is 38 kcal/mol less stable. From an energetic point of view, mechanism **A** is thus much more favorable than variant **B**. What can further help to dismiss mechanism **B** is a consideration of the relative intensities of the fragment ions in the MI and CA experiments performed on alkyloxalates (Table 4) as well as the energy demands of the various fragments (Table 6). Decarboxylation dominates all spectra, what has been in part explained by a most favorable thermochemistry of the products obtained as compared to those obtained from decarboxylation and simultaneous decarboxylation and decarboxylation. Nevertheless, this dissociation requires the passage through a transition structure, whereas the two other dissociations pathways are direct bond cleavages, which most likely require no excess activation energies. Thus, if the transition structure associated with decarboxylation were energetically extremely demanding, the alkyloxalate ions would not be able to cross it particularly in the MI process and the other dissociation pathways would be accordingly more present. Therefore, the transition structures TS_{A} , which are similar in energy to the resulting products, seems to be highly favored in the course of dissociation of alkyloxalates. By comparing the experimental results with the energies predicted for TS_{A} and TS_{B} , we conclude that decarboxylation occurs through a mechanism of type **A**. The optimized structures of both INC_{A} and TS_{A} and of are presented in Fig. 6 for each alkylcarbonates **1–5**.



Scheme 6. Two mechanistic variants for the decarboxylation of alkyloxalates ROCOCO^- ($\text{R} = \text{H}, \text{CH}_3, \text{C}_2\text{H}_5, i\text{-C}_3\text{H}_7, \text{and } t\text{-C}_4\text{H}_9$).

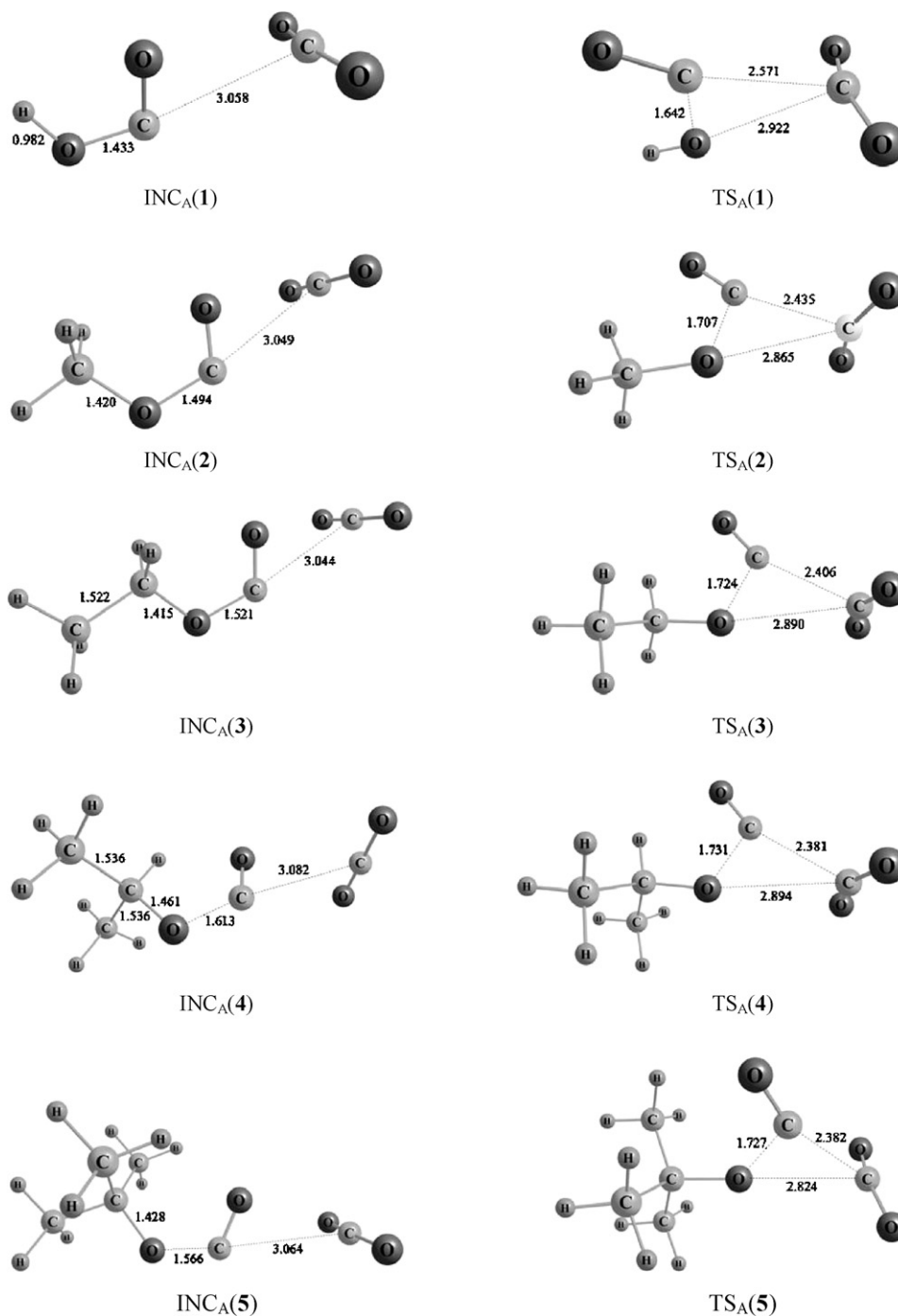


Fig. 6. Optimized structures of the ion–neutral complexes INC_A and the transition structures TS_A for the five alkyloxalates under study at the MP2/6-311++G(d) level of theory.

4. Conclusions

The different conformers of alkyloxalates $ROCOCOO^-$ are investigated computationally for $R = H, CH_3, C_2H_5, i-C_3H_7,$ and $t-C_4H_9$. The results show that the most stable conformers differ according to the substituent R ; due an intramolecular hydrogen bond, the hydrogen oxalate ion **1** is most stabilized in a planar cC conformation, whereas a *trans* (T) conformation between the two carbonyl groups is preferred for the larger substituents. The favorable spatial position of the substituents

also differs with R . The most stable conformation with respect to rotation around the $O_{(4)}-C_{(2)}$ bond is *cis* for $R = H, CH_3,$ and C_2H_5 , whereas the *trans* conformation is favored for $R = i-C_3H_7$ and $t-C_4H_9$. Further, alkyloxalates anions have been submitted to MI and CA experiments in order to investigate their unimolecular and their collision-induced dissociation behavior. The results are similar for all substituents and three decomposition pathways are observed: decarbonylation, decarboxylation, and simultaneous decarboxylation and decarbonylation. The first pathway is by far the dominant decomposition process

observed in both MI and CA experiments, which is also confirmed from a thermochemical point of view. Loss of CO leads to the formation of alkylcarbonates ROCOO^- , whereas elimination of CO_2 leads to alkoxy carbonyl anions ROCO^- , and the combined production of CO and CO_2 affords the corresponding alkoxy anions RO^- . While the two latter decomposition paths correspond to direct bond cleavages, decarbonylation requires a rearrangement of the anions, which is suggested to proceed via the formation of an intermediate ion–neutral complex.

Acknowledgements

This work was supported by the Deutsche Forschungsgemeinschaft and the Fonds der Chemischen Industrie. We thank the Institut für Mathematik of the Technische Universität Berlin and the Norddeutscher Verbund für Hoch- und Höchstleistungsrechnen (HLRN) for the generous allocation of computer time.

References

- [1] J.H. Bowie, *Mass Spectrom. Rev.* 9 (1990) 349.
- [2] C.A. Schalley, D. Schröder, H. Schwarz, *Int. J. Mass Spectrom. Ion Processes* 153 (1996) 173.
- [3] W.J. Richter, H. Schwarz, *Angew. Chem. Int. Ed. Engl.* 17 (1978) 424.
- [4] Y.L. Guo, J. Grabowski, *Int. J. Mass Spectrom. Ion Processes* 117 (1992) 299.
- [5] D. Schröder, H. Soldi-Lose, H. Schwarz, *Aust. J. Chem.* 56 (2003) 443.
- [6] C. Møller, M.S. Plesset, *Phys. Rev.* 46 (1934) 618.
- [7] T. Clark, J. Chandrasekhar, G.W. Spitznagel, P.V.R. Schleyer, *J. Comput. Chem.* 4 (1983) 294.
- [8] R. Krishnan, J.S. Binkley, R. Seeger, J.A. Pople, *J. Chem. Phys.* 72 (1980) 650.
- [9] M.J. Frisch, G.W. Trucks, H.B. Schlegel, G.E. Scuseria, M.A. Robb, J.R. Cheeseman, J.A. Montgomery Jr., T. Vreven, K.N. Kudin, J.C. Burant, J.M. Millam, S.S. Iyengar, J. Tomasi, V. Barone, B. Mennucci, M. Cossi, G. Scalmani, N. Rega, G.A. Petersson, H. Nakatsuji, M. Hada, M. Ehara, K. Toyota, R. Fukuda, J. Hasegawa, M. Ishida, T. Nakajima, Y. Honda, O. Kitao, H. Nakai, M. Klene, X. Li, J.E. Knox, H.P. Hratchian, J.B. Cross, V. Bakken, C. Adamo, J. Jaramillo, R. Gomperts, R.E. Stratmann, O. Yazyev, A.J. Austin, R. Cammi, C. Pomelli, J.W. Ochterski, P.Y. Ayala, K. Morokuma, G.A. Voth, P. Salvador, J.J. Dannenberg, V.G. Zakrzewski, S. Dapprich, A.D. Daniels, M.C. Strain, O. Farkas, D.K. Malick, A.D. Rabuck, K. Raghavachari, J.B. Foresman, J.V. Ortiz, Q. Cui, A.G. Baboul, S. Clifford, J. Cioslowski, B.B. Stefanov, G. Liu, A. Liashenko, P. Piskorz, I. Komaromi, R.L. Martin, D.J. Fox, T. Keith, M.A. Al-Laham, C.Y. Peng, A. Nanayakkara, M. Challacombe, P.M.W. Gill, B. Johnson, W. Chen, M.W. Wong, C. Gonzalez, J.A. Pople, *Gaussian 03, Revision C. 02*, 2004.
- [10] A.P. Scott, L. Radom, *J. Phys. Chem.* 100 (1996) 16502.
- [11] M.J. Frisch, J.A. Pople, J.S. Binkley, *J. Chem. Phys.* 80 (1984) 3269.
- [12] C.W. Bock, R.L. Redington, *J. Chem. Phys.* 85 (1986) 5391.
- [13] J. Higgins, X. Zhou, R. Liu, T.T.S. Huang, *J. Phys. Chem. A* 101 (1997) 2702.
- [14] A. Mohajeri, N. Shakerin, *J. Mol. Struct.* 711 (2004) 167.
- [15] M. Remko, K.R. Liedl, B.M. Rode, *J. Chem. Soc., Perkin Trans. 2* (1996) 1743.
- [16] J. Tyrrell, *J. Mol. Struct. (THEOCHEM)* 258 (1992) 389.
- [17] C. Van Alsenoy, V.J. Klimkowski, L. Schafer, *J. Mol. Struct. (THEOCHEM)* 109 (1984) 321.
- [18] C. Cheng, S.-F. Shyu, *Int. J. Quantum Chem.* 76 (2000) 541.
- [19] K. Levsen, H. Schwarz, *Mass Spectrom. Rev.* 2 (1983) 77.
- [20] J. Langlet, J. Caillet, M. Allavena, V. Raducu, B. Gauthier-Roy, R. Dahoo, L. Abouaf-Marguin, *J. Mol. Struct.* 484 (1999) 145.
- [21] J.S. Muentner, R. Bhattacharjee, *J. Mol. Spectrosc.* 190 (1998) 290.
- [22] S. Peppe, S. Dua, J.H. Bowie, *J. Phys. Chem. A* 105 (2001) 10139.
- [23] R.W. Randall, J.P.L. Summersgill, B.J. Howard, *J. Chem. Soc., Faraday Trans. 86* (1990) 1943.
- [24] Y. Xu, A.R.W. McKellar, B.J. Howard, *J. Mol. Spectrosc.* 179 (1996) 345.
- [25] V. Raducu, B. Gauthierroy, R. Dahoo, L. Abouafmarguin, J. Langlet, J. Caillet, M. Allavena, *J. Chem. Phys.* 102 (1995) 9235.
- [26] D. Schröder, H. Schwarz, S. Dua, S.J. Blanksby, J.H. Bowie, *Int. J. Mass Spectrom.* 188 (1999) 17.
- [27] R.N. Hayes, R.J. Waugh, J.H. Bowie, *Rapid Commun. Mass Spectrom.* 3 (1989) 338.
- [28] P.C.H. Eichinger, J.H. Bowie, *Int. J. Mass Spectrom. Ion Processes* 123 (1991) 110.
- [29] H. Soldi-Lose, D. Schröder, H. Schwarz, *Int. J. Mass Spectrom.*, to be submitted.
- [30] R.A.J. O'Hair, J.H. Bowie, R.N. Hayes, *Rapid Commun. Mass Spectrom.* 2 (1988) 275.
- [31] S.T. Graul, R.R. Squires, *J. Am. Chem. Soc.* 110 (1988) 607.
- [32] D. Schröder, M. Semialjac, H. Schwarz, *Eur. J. Mass Spectrom.* 9 (2003) 287.
- [33] T.M. Ramond, G.E. Davico, R.L. Schwartz, W.C. Lineberger, *J. Chem. Phys.* 112 (2000) 1158.
- [34] N. Heinrich, H. Schwarz, in: J.P. Maier (Ed.), *Ion and Cluster-Ion Spectroscopy and Structure*, Elsevier, Amsterdam, 1989, p. 329.
- [35] K. Banholzer, H. Schmid, *Helv. Chim. Acta* 39 (1956) 548.
- [36] W.W. Elliott, D.L. Hammick, *J. Chem. Soc.* (1951) 3402.
- [37] P.C.H. Eichinger, R.N. Hayes, J.H. Bowie, *J. Chem. Soc., Perkin Trans. 2* (1990) 1815.